International Journal of Optomechatronics

ISSN: 1559-9612 (Print) 1559-9620 (Online) Journal homepage: http://www.tandfonline.com/loi/uopt20

Apnea Detection Method for Cheyne-Stokes Respiration Analysis on Newborn

Taiga Niimi , Yushi Itoh , Michiya Natori & Yoshimitsu Aoki

To cite this article: Taiga Niimi , Yushi Itoh , Michiya Natori & Yoshimitsu Aoki (2013) Apnea Detection Method for Cheyne-Stokes Respiration Analysis on Newborn, International Journal of Optomechatronics, 7:2, 67-82, DOI: 10.1080/15599612.2012.762567

To link to this article: https://doi.org/10.1080/15599612.2012.762567

Published online: 08 May 2013.

International Journal of Optomechatronics, 7: 67–82, 2013

ISSN: 1559-9612 print/1559-9620 online
DOI: 10.1080/15599612.2012.762567

Taylor & Francis
Taylor & Francis Group

APNEA DETECTION METHOD FOR CHEYNE-STOKES RESPIRATION ANALYSIS ON NEWBORN

Taiga Niimi,[1] Yushi Itoh,[2] Michiya Natori,[2] and Yoshimitsu Aoki[1]

[1]*Department of Science and Engineering, Keio University, Kanagawa, Japan*
[2]*National Center for Child Health and Development, Tokyo, Japan*

Cheyne-Stokes respiration is especially prevalent in preterm newborns, but its severity may not be recognized. It is characterized by apnea and cyclical weakening and strengthening of the breathing. We developed a method for detecting apnea and this abnormal respiration and for estimating its malignancy. Apnea was detected based on a "difference" feature (calculated from wavelet coefficients) and a modified maximum displacement feature (related to the respiratory waveform shape). The waveform is calculated from vertical motion of the thoracic and abdominal region during respiration using a vision sensor. Our proposed detection method effectively detects apnea (sensitivity 88.4%, specificity 99.7%).

Keywords: apnea, Cheyne-Stokes respiration, FG vision sensor, image processing, newborn, preterm, respiratory monitoring system, signal processing, wavelet

1. INTRODUCTION

The rate of low-birth-weight neonates has been increasing in recent years. Low birth weight (<2500 g) is caused by preterm birth or intrauterine agenesis. The death rate among these infants is high because their bodily and respiratory functions are immature. Diseases marked by abnormal respiration are prevalent in preterm neonates. They include newborn respiratory distress syndrome, apnea attacks, and sudden infant death syndrome (SIDS). As the gestational age decreases, these diseases become more conspicuous. Respiratory monitoring of newborns is imperative because it enables both early diagnosis and prevention of various diseases. Early discovery of a disorder and estimation of the state of respiratory function can provide proper medical treatments during early stages of the disease. We believe that respiratory monitoring is a significant factor in saving newborns' lives.

Neonatal respiration is monitored in neonatal intensive care units by means of two respiratory contact-type sensors. The first sensor is a cardiorespiratory monitor that measures the respiratory rate and the heartbeat. This sensor uses stick-on electrodes that are attached to the body. It measures changes of impedance when slight electrical current is applied to the electrodes, thereby detecting chest and abdominal movement.

Address correspondence to Yoshimitsu Aoki, 24th Building, 3F, Room 307 Keio University, 3-14-1, Hiyoshi, Kohoku-ku, Yokohama-Shi, Kanagawa, 223-8522 Japan. E-mail: aoki@elec.keio.ac.jp

NOMENCLATURE

h	distance between screen and the lens of FG vision sensor	$x(t)$	signal of respiratory waveform
		a	scale parameter
l	focal point distance of CCD camera	b	time parameter
d	base length of FG sensor	w	wavelet coefficient
δ	displacement vector of the spot on 2-D CCD array between frames	j, k	parameters of discrete wavelet transform
dZ, dX, dY	displacement of spot on the surface of object between frames	MMD	value of modified maximum displacement
x, y	the position of spot on the 2-D CCD array	W_{max}	maximum sequence value calculated from wavelet coefficient
t	times	W_{middle}	middle sequence value calculated from wavelet coefficient
$\psi(t)$	wavelet function		

The second sensor is a pulse oximeter that measures the blood oxygen saturation level (SpO_2) indirectly. It has a pair of small light-emitting diodes (LEDs) facing a photodiode through a translucent part of the patient's body, usually a fingertip or an earlobe. One LED is red, and the other is infrared. Absorption at these wavelengths differs between oxyhemoglobin and its deoxygenated form. SpO_2 can then be calculated from the ratio of the absorption of the red and infrared lights. However, these respiratory contact-type sensors may cause a skin irritation because of the newborn's sensitivity. They may also obstruct access to the patient and are often removed for application of medical treatments or because of the baby's movements. The accuracy of detection is different when the location of the sensor's attaching portion changes.

Cheyne-Stokes respiration (CSR) is abnormal respiration characterized by cyclical and gradual changes in breath strength between periods of apnea and normal breathing. The most severe state of periodic breathing, CSR has been defined by the presence of at least three consecutive apneic periods of at least 3 seconds each separated by intervals of $\leq$20 seconds (Kelly and Shannon 1979). CSR is controlled by the part of the brain that controls respiratory function. Individuals in the midst of a CSR attack cannot respond or react quickly enough to changes in oxygen or carbon dioxide levels in the bloodstream.

The CSR is triggered by a hypoxic state associated with hypoventilation (Rigatto and Brady 1972), which occurs because the respiratory control of the immature central nerve of respiratory function is unstable. Therefore, CSR is highly prevalent in newborns, especially those who were born before term and whose central nervous system is immature. CSR is closely related to the maturity of the respiratory function of preterm newborns (Oliveira et al. 2004). For this reason, estimating the severity of CSR can inform us of the patient's respiratory function. Also, CSR analysis has the potential to discover diseases at an early stage [e.g., excessive amounts of periodic breathing in infants with near-miss SIDS (Kelly and Shannon 1979; Shannon, Carley, and Kelly 1988)] and to contribute to our knowledge of the respiratory physiology of newborns. CSR has not been studied broadly in newborns. Reports in the signal-processing literature are especially sparse because of the disadvantages of having to use respiratory contact-type sensors. Thus, researchers have not been able to obtain sufficient data for fear of imposing a burden on preterm babies and those with CSR. Also, as already noted, detection accuracy of respiratory contact-type sensors is unstable.

To solve these problems, we developed a respiratory monitoring system for newborns using an FG Vision Sensor (Kurami et al. 2011). This device is an active stereo three-dimensional (3-D) sensor that can be used for noncontact 3-D measurements (Nakazawa, Nakajima, and Kobayashi 1986). The system can calculate more accurate respiratory waveforms than can traditional medical sensors. With the aid of this system, we aimed at developing a novel detection method for estimating the severity of CSR.

This article is organized as follows. Related studies are described in Section 2. A respiratory monitoring system is described in Section 3. In Section 4, we explain a method for detecting apnea. The experiment is presented in Section 5. Our conclusions and plans for future work are described in Section 6. Our apnea detection method offers four main contributions: apnea analysis, CSR detection, estimation of CSR severity, and learning more about the respiratory physiology of newborns.

2. RELATED STUDIES

Some waveform analysis-based studies have described the classification methods of CSR for cardiac failure (Garde et al. 2008; Garde et al. 2011). One of these studies showed classification results of waveforms by analyzing the frequency of the envelope curve. The classification accuracy of the method exceeds 80% for adults, whose waveforms are more stable than those of newborns. The respiratory state of newborns changes frequently over a short time, and the envelope curve is distorted. Thus, using the frequency of the envelope curve for detecting CSR in a newborn would likely problematic. We therefore focused on apnea and developed a new apnea detection method, which will help with CSR detection and the estimation of CSR severity.

Apnea is commonly seen in preterm newborns. It is considered a clinical event if it lasts >10 seconds and is accompanied by either bradycardia <80 beats per minute or desaturation of oxygen below 80% (Finer et al. 2006). In this case, apnea is a clinical event that requires prompt medical attention.

Traditional methods for apnea detection include artificial neural network (ANN)-based methods with signals of polysomnography (PSG). PSG is a multichannel recording instrument that uses contact-type sensors during the entire sleeping process, including electroencephalography, electrooculography, electromyography, nasal airflow (NAF), abdominal and/or thoracic movements, body position, snore microphone, electrocardiography, and blood oxygen saturation (SaO_2) (Chesson et al. 1997). These methods detect apnea whose duration is >10 seconds for sleep apnea syndrome (Varady et al. 2002; Tian and Liu 2005; Fontenla-Romero et al. 2005) by using PSG signals such as NAF and SaO_2, among others. The sampling rate of PSG signals is normally >100 Hz. These methods down-sample the rates of the signals and apply windowing to those signals for ANN. However, signals for ANN in case of a PSG signal >30 Hz have more information than those of respiratory waveforms calculated by our system, which are only 8 Hz (explained later). Therefore, we cannot apply these methods to signals in our system.

Also, the direction of the traditional methods explained above is different from that of our method. We focus on not only clinical apnea but also apnea of <10 seconds to study the respiratory physiology of newborns. CSR in infants has apnea of not only >10 seconds but also apnea of 1–10 seconds despite its definition. Respiratory analysis containing this shorter apnea can contribute to knowledge of respiratory physiology of newborns.

There is yet another method for apnea detection that depends on use of the standard deviation (Lee et al. 2012). This method uses chest impedance (CI) signals. It first removes the heart rate signal component, which appears during periods of apnea of the CI signal, by resampling the CI signal with an equal number of steps in each RR interval (filtered CI). For the first step, this method makes a histogram of the standard deviation at every quarter second for a 2-second interval at the middle. Next, it calculates two distributions corresponding to the deviation histogram of apnea periods and respiratory periods, respectively. Then, it calculates the apnea probability value from the values of these distributions corresponding to the calculated standard deviation. Although the accuracy of this method is >90%, it ignores all apnea periods of <2 seconds and <5 seconds unless the event was within 5 seconds of another event. Furthermore, our apnea definition is that the apnea has a wave height of <0.1 mm and it continues >1.0 second (explained later). It is difficult to set parameters for the method to detect apnea whose wave height is specified in our definition.

Recent studies on apnea detection for adults have utilized frequency energy calculated by fast Fourier transform (FFT) (Nakano et al. 2007) or the shape of the waveform (van Houdt et al. 2011). FFT needs a fixed comparatively long time (window) to extract correct frequency information from the waveform. However, the sampling rate of the monitoring system is 8 Hz and the length of the apnea we defined for a newborn baby is at least 1.0 second (explained later). Therefore, this method, which is used for adults, is not proper for monitoring the respiratory waveform of a newborn. Also, the waveform can be distorted when respiration is unstable. Unstable respiration can distort the results of a waveform shape-based method.

Considering those facts, information on the shape of the waveform alone or information on frequency alone does not confer enough robustness. Therefore, we selected a feature related to the height of the waveform and a feature of wavelet transform (WT).

3. RESPIRATORY MONITORING SYSTEM

3.1. System Recapitulation

The respiratory monitoring system is composed of an FG Vision Sensor and an operational component that calculates the respiratory waveform (Figure 1(*a*)). For calculating the latter, the FG Vision Sensor is positioned above the newborn.

The FG Vision Sensor is composed of a spot projector and an infrared charge-coupled device (CCD) camera. The spot projector is composed of a diffraction grating of an optical fiber (fiber grating) and an infrared laser. When a laser is vertically entered into the fiber grating, the spot is irradiated on the screen net, similar to a square lattice.

The spot image is obtained by taking a picture of the screen with the infrared CCD camera (Figure 1(*b*)). When the depth of the spot irradiation position changes, the coordinate value of the spot changes in a constant direction. It is then possible to calculate the displacement vector of the spot irradiation position from the displacement vector of the spot on the two-dimensional (2-D) CCD array. With this scheme,

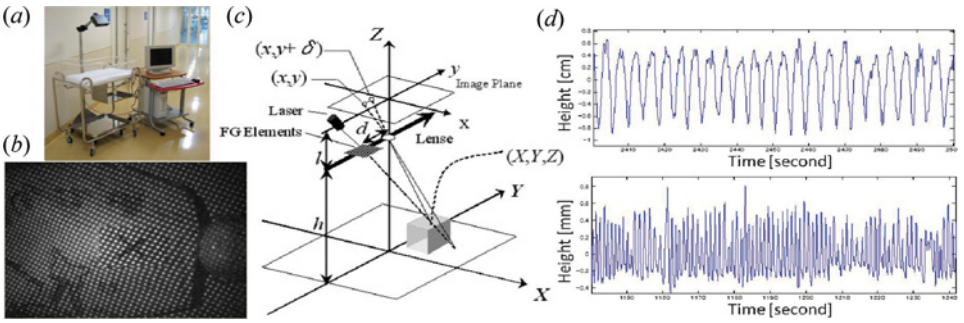

Figure 1. (*a*) System appearance, (*b*) spot image, (*c*) optical layout of FG Vision Sensor, (*d*) respiratory waveform. *Top*: adult; *bottom*: newborn (color figure available online).

it then calculates the 3-D displacement vector of the spot irradiating the thoracic and abdominal region and calculates the respiratory waveform (Kurami et al. 2011).

3.2. Spot Displacement Vector Calculation

To detect the thoracoabdominal movement with respiration, the system calculates the displacement vector of each spot. Figure 1(*c*) shows the optical layout of the FG Vision Sensor. The parameter h is the distance between the screen and the lens. Parameter l is the focal point distance of the CCD camera. Parameter d is the base length, which is the distance between the center of the lens and that of the fiber grating. Parameter δ is the displacement vector of the spot on 2-D CCD array between frames. Calculation of the displacement vector of each spot is based on optical triangulation, as shown in Equations (1)–(3):

$$dZ = h^2\delta/(dl + h\delta) \tag{1}$$

$$dX = x(h - dZ)/l \tag{2}$$

$$dY = (y + \delta)(h - dZ)/l \tag{3}$$

3.3. Respiratory Waveform

A respiratory waveform is calculated using the z-axial displacement vector. We calculated the average value of the vectors in the thoracoabdominal region. This average value is the velocity of the thoracoabdominal region between frames. The sum of all velocities obtained in each frame is the thoracoabdominal height. This system convolves the waveform with a bandpass filter whose frequency scale is 0.17–2.0 Hz—the respiratory frequency band of a newborn.

Figure 1(*d*) shows results for 100 seconds of a respiratory waveform of an adult and a newborn calculated by the described system. The adult breathing rhythm is about 15–20 breaths per minute, whereas that of newborns is about 30–120 breaths per minute. The typical respiratory waveform height of a newborn is 0.1–1.0 mm, with the waveform being unstable for varied respiration over a short term.

The system monitors neonatal respiration and detects apnea in real time. It sets off an alarm when the detected apneic period is longer than 20 seconds because longer-duration apnea could result in certain death of the infant (Kurami et al. 2011). The system also detects nonbreathing movements of newborns. The preterm newborn almost never initiates body movements. If a newborn moves, the average value of the displacement vectors on the thoracoabdominal region becomes much larger than that of breathing movements. Thus, it is easy to detect body motion from waveforms.

4. APNEA DETECTION

A physician at the National Center for Child Health and Development (NCCD) with whom we collaborate monitored the motion of the thoracoabdominal region of newborns during respiration. At the same time, he monitored signals from our system and signals from the monitoring system used at the NCCD. Through this collaboration, we were able to establish that apnea has a wave height of <0.1 mm and that it continues for >1.0 second, giving it physiological meaning.

4.1. Previous Apnea Detection Method

The monitoring system requires real-time processing to determine that a patient is in danger as rapidly as possible. We adopted a simple method for this purpose. The system calculates the maximum displacement of the respiratory waveform during the prior 1.0 second up to the present time (Figure 2(*a*)). When the value is less than a threshold 0.1 mm and the state continues for at least 1.0 second, the monitoring system regards it as a period of apnea. Although the accuracy of this method exceeds 70%, it cannot respond to unstable respiration. When respiration is unstable, the calculated waveform contains intermittently high and low values because the thoracoabdominal movement with respiration is not orderly. Consequently, the system gives false-positive and false-negative readings. Also, false-positive recordings are generated when the period around the ending point of expiration and the starting point of inspiration exceeds 1.0 second. We have attempted to develop a method to provide a detailed analysis of CSR respiration for offline processing. For this purpose, however, the apnea detection method must realize higher accuracy.

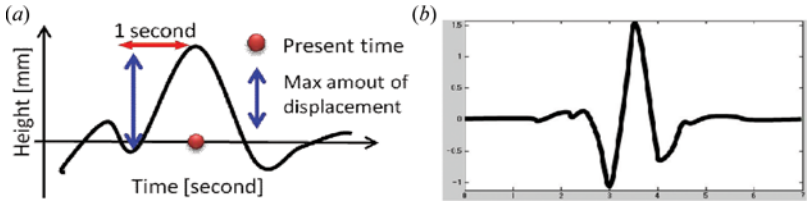

Figure 2. (*a*) Maximum amount of displacement of the respiratory waveform during the last 1.0 second from the present time. (*b*) Symlet4 wavelet (color figure available online).

4.2. Orthonormal Wavelet Transform

WT is one of the time-frequency analyses that determines the proper time and frequency resolution. Equation (4) shows wavelet function. The frequency scale of the wavelet can be altered by changing the scale parameter a, and the width of the wavelet can be changed to the optimal width for the band of frequencies at the same time. Equation (5) shows that WT is to convolve the waveform with the wavelet. The results of the transform are called the "wavelet coefficient,"

$$\psi_{a,b}(t) = \psi\left(\frac{t-b}{a}\right)\Big/\sqrt{a} \tag{4}$$

$$w_{a,b} = \int_{-\infty}^{\infty} x(t)\psi_{a,b}(t)dt, \tag{5}$$

where a is the scale parameter, b is the time parameter, and $x(t)$ is the respiratory waveform. We adopted an orthonormal wavelet for the fast WT.

Equation (6) shows orthonormal wavelet function. The parameters of an orthonormal wavelet are proportional to a factor of 2:

$$\psi_{j,k}(t) = 2^{-j/2}\psi(2^{-j}t - k) \tag{6}$$

where $a = 2^j$, $b = 2^j k$, and j is the resolution level. If the value j increases, the wavelet frequency scale makes the shift to a lower frequency. The sampling rate of the monitoring system is 8 Hz, and the breathing cycle of newborns is about 0.5–2.0 seconds. Hence, the wavelet resolution levels we adopted were 2, 3, and 4. The frequency range of each resolution level was 1–2 Hz, 0.5–1.0 Hz, and 0.25–0.50 Hz, respectively.

The advantage of the fast WT is that its computational cost is low because we can calculate wavelet coefficients of other resolution levels from that of level 1. Moreover, the wavelet of each resolution level extracts frequency information from a local range of waveforms in the time axis compared with FFT. The frequency energy of a wavelet contains less extra frequency energy of the respiratory period around the apnea than that of FFT. In the case of the wavelet, the influence of the extra frequency energy of the respiratory period corresponds with the width of the wavelet's time window, whose level of resolution corresponds with the respiratory frequency. On the other hand, the influence of the extra frequency energy of FFT corresponds to the width of the fixed long-time window, which corresponds to the respiratory frequency band—and the energy value is larger than that of wavelet. Therefore, around the short apnea period, the frequency energy of the wavelet contains less respiratory frequency energy compared with that with FFT. We adopted the Symlet4 wavelet (Figure 2(*b*)), which has a comparatively symmetrical waveform to match changes in the height of the respiratory waveform and in the wavelet coefficient temporally.

4.3. Proposed Method

Our method uses two features for apnea detection: the difference feature and the MMD feature. The difference feature is calculated from wavelet coefficients.

The MMD is related to the shape of respiratory waveform. Our method has two conditions using these features for apnea detection, with the result (the apnea label) being determined by combining the results from the two conditions.

4.3.1. Difference feature. We propose that the difference feature is a main factor for apnea detection. It is the difference between the maximum and middle sequence values calculated from wavelet coefficients of the respiratory waveform. When it is used for apnea detection, it is superior to the respiratory frequency energy of the FFT and the WT. The frequency energy of the respiratory frequency band is typically used in some frequency-based methods for detecting apnea. During respiration, the respiratory frequency is constant, and the frequency energy calculated from FFT and WT is larger than its threshold. In contrast, apnea has little frequency energy from the respiratory frequency band. In this case, the respiratory frequency energy is lower than its threshold, and frequency-based method can detect apnea.

The respiratory frequency energy, however, does not tend to decrease with short apnea but is lower around the borders between the apnea period and neighboring respiratory periods. There are two reasons for this: (1) The local waveform around transition of the respiratory states (apnea $\rightarrow$ breath) has wideband frequency energy. (2) FFT and WT have time windows and extract extra frequency energy from neighboring respiratory periods around the apnea.

For this problem, we found that our difference feature is useful for apnea detection. During respiration, the respiratory frequency exists in one specific frequency band. The absolute value of the difference has almost the same value of the respiratory frequency energy and is larger than its threshold. This feature can diminish with shorter-duration apneas and decrease around the borders between the apnea and neighboring respiratory period. This is the reason that the frequency energy values of the frequency bands have different values in the short-duration apneas and during transition of the respiratory state.

We calculated the difference feature with the wavelet because, comparatively, the wavelet has less impact from its time window than in the case of FFT. First, we adapted the fast WT to a respiratory waveform and calculated the wavelet coefficient at each resolution. Second, we adapted a spline interpolation to each wavelet-level coefficient sequence because time coefficients of orthonormal wavelets are discrete values. These three-level wavelet coefficients at each time are squared, as in Figure 3(*a*). Those squared values are reassigned to three new sequences: maximum, middle, and minimum sequence values, as in Figure 3(*b*). The maximum sequence value is composed of values that are the maximum squared coefficients of the three wavelet levels at each time. The difference feature is the difference between the maximum and middle sequence values.

During respiration, respiratory frequency is constant within the local range of the waveform on its time axis. In this case, the maximum sequence value has almost the same as the respiratory frequency energy, and the difference feature is almost equal to the respiratory frequency energy. Our target apnea period is >1.0 second. The values of features for detecting apnea must decline beyond its threshold not only for long apnea but also for short apnea. The difference feature can satisfy this requirement because it becomes lower than the maximum sequence value when its time is within the apnea period. The difference feature in the vicinity of the borders

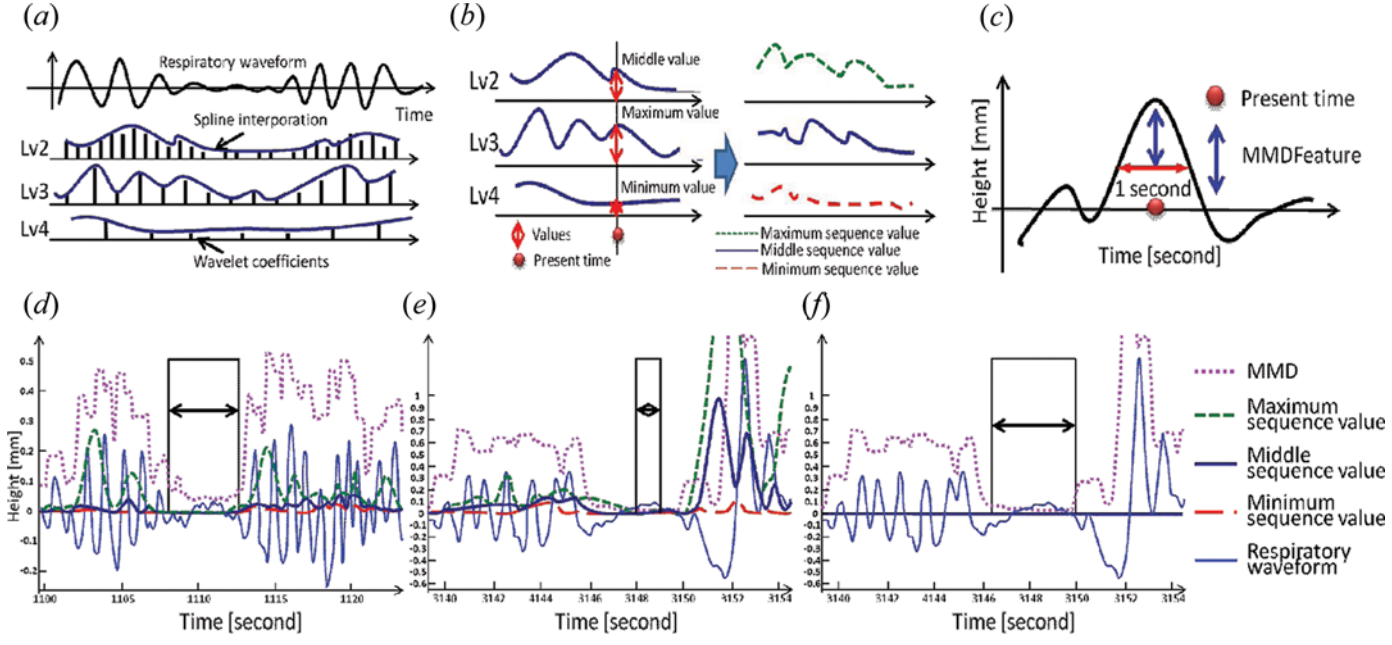

Figure 3. Apnea detection method. (*a*) Wavelet coefficients of three levels of resolution are squared at each time and then applied with a spline interpolation. (*b*) These interpolated wavelet coefficients at each time are compared with each other (absolute values). According to their value, they are reassigned to three new sequences, which include maximum, middle, and minimum sequence values. (*c*) Maximum displacement (MMD) of the respiratory waveform in 1.0 second around the middle of a given time. (*d*) A result of apnea detection with (7), (8), and (9). Black rectangle indicates detected apnea. (*e*) In the case of the respiratory volume not diminished around the period of apnea, (7), (8), and (9) cannot detect the whole apnea area. (*f*) Apnea can be detected only with the MMD feature in the case of (*e*) (color figure available online).

between the apnea period and its neighboring respiratory period diminishes because not only the maximum sequence value has frequency energy but the middle sequence value has it as well.

4.3.2. MMD feature. Although the value of the difference feature can be lower around the borders between apnea and its neighboring respiratory period, the wavelet coefficient could also have a low value because of its dependence on the shape of the waveform. This situation leads to a false-positive result. It is also difficult to detect apnea whose wave height is <0.1 mm. To solve this problem, we sampled the maximum displacement (MMD) of the respiratory waveform in 1.0 second around the middle of a given time (Figure 3(*c*)). This feature is modified from the previous method.

4.3.3. Apnea condition. We have mainly adopted the difference feature, the maximum sequence value, and the MMD to prevent false-positive errors. We call this combination the "wavelet-based method."

$$\mathrm{MMD} < 0.125 \tag{7}$$

$$\mathrm{W}_{\max} < 0.05 \tag{8}$$

$$\mathrm{W}_{\max} - \mathrm{W}_{\mathrm{middle}} < 0.015 \tag{9}$$

where $\mathrm{W}_{\max}$ is the maximum sequence value, and $\mathrm{W}_{\mathrm{middle}}$ is the middle sequence value.

Figure 3(*d*) shows that apnea is detected with these three features. The respiratory volume is decreased, the values of the features are lower around the apnea, and the entire apnea period is detected. However, if the respiratory volume is not low around the apnea period, these features sometimes cannot detect apnea because of the existence of frequency energy around the borders between apnea and its neighboring respiratory periods (Figure 3(*e*)). On the other hand, Figure 3(*f*) shows that all of the apnea can be detected with the MMD feature alone. However, 1.0- to 1.5-second periods of apnea detected by MMD are eliminated because there are a number of false-positive errors. We believe that this MMD method is comparable to the wavelet-based method.

$$\mathrm{MMD} < 0.1 \tag{10}$$

The wavelet-based method and the MMD method compensate for each other's weaknesses. The former never suffers from unstable respiration with wavelets and MMD. It can detect apnea stably. However, it is not valid in cases such as that in Figure 3(*e*). On the other hand, although the latter can work well in such cases, it suffers from unstable respiration. Therefore, our proposed method provides answers that are the combined results (apnea label) of the wavelet-based method and the MMD method.

4.3.4. Experiment. For comparison, we designed a condition for apnea detection with FFT instead of WT. An FFT of the waveform was used to obtain the short-time power spectrum within the respiratory frequency band. This power spectrum was designated FFT power. The time window used for FFT was the Hanning window of 80 points (10 seconds). The bandwidth of respiratory frequency was set at 0.5–2.0 Hz (30–120 cycles/min). FFT was performed at every point (overlapped windows). This step makes an ''FFT power–time series.'' We designed a condition for apnea detection with an MMD method and FFT-based method that was modified from the wavelet-based method to compare this condition with our method. We called it the FFT approach. The modified part of the condition is below.

$$\text{FFT power} < 9 \tag{11}$$

Equation (11) is used in place of Equations (8) and (9) of our method. We empirically determined thresholds of our method on the basis of a doctor's assessment of the results of apnea detection.

We compared the accuracy of detecting apnea using a previous method, the FFT approach, and our proposed method. We collected data for 0.4–1.0 hour on the respiratory waveforms of 11 newborns. Before the experiment, we determined the correct values for apnea based on information from a doctor's lectures. Our method depends on a number of parameters. Therefore, we cannot evaluate the performance of our method by a receiver operating characteristics curve. Hence, we empirically determined thresholds of our method on the basis of a doctor's assessment of the results of apnea detection. Table 1 shows the sensitivity and specificity of the previous method, the FFT approach, and the proposed method for each newborn. Table 2 shows the details of Table 1. True positive means that the method correctly identified apnea. This value is expressed by the number of apneic events. The number of correct apneic events was 924. False negative is also expressed by the number of apneic events. True negative values show if the method has correctly identified the periods that were not apneic. This value is expressed in units of time. False-positive values are also expressed as time.

In the experimental results (Figures 4(*a*) and 4(*b*)), the section with a value of 0.5 shows the results of the proposed method. The section with a value of 1.0 shows the results of the previous method. The section with a value of 0.25 shows the results of the FFT approach. In Figure 4(*a*), the proposed method decreased the number of false-positive results, which may have been caused when the period around the ending point of expiration and the starting point of inspiration exceeded 1.0 second,

Table 1. Accuracy comparisons among the previous method, FFT-based method, and proposed method

Method	TP	FN	FP	TN	Sens (%)	Spec (%)
Previous	748	176	372.4	30081.6	81	98.8
FFT	757	167	208.3	30245.7	81.9	99.3
Proposed	817	107	91.3	30362.7	88.4	99.7

Table 2. Details of the accuracy of the previous method, FFT-based method, and proposed method

Previous method	Correct TP	Correct TN (times)	TP	FN	FP	FP (times)	Sens	Spec
Pa1	37	1457.9	30	7	26	42.5	81.1	97.1
Pa2	72	3286.6	53	19	9	11.5	73.6	99.7
Pa3	37	1089.0	30	7	8	19.9	81.1	98.2
Pa4	87	3646.9	72	15	11	20.6	82.8	99.4
Pa5	143	3335.9	97	46	43	65.4	67.8	98.0
Pa6	113	3686.3	108	5	68	129.1	95.6	6.5
Pa7	92	32701.0	82	10	6	10.6	89.1	99.7
Pa8	17	2998.8	8	9	0	21.5	47.1	99.3
Pa9	44	1555.3	31	13	6	17.1	70.5	98.9
Pa1	28	2700.0	20	8	2	1	71.4	100.0
Pa11	254	2136.4	217	37	19	33.1	85.4	98.4
Total	*924*	*30454.0*	*748*	*176*	*198*	*372.4*	*81*	*98.8*
FFT approach	Correct TP	Correct TN (times)	TP	FN	FP	FP (times)	Sens	Spec
Pa1	37	1457.9	33	4	19	32.0	89.2	97.8
Pa2	72	3286.6	59	13	11	18.8	81.9	99.4
Pa3	37	1089.0	32	5	10	13.5	86.5	98.8
Pa4	87	3646.9	69	18	9	11.1	79.3	99.7
Pa5	143	3335.9	115	28	26	36.1	80.4	98.9
Pa6	113	3686.3	91	22	35	51.1	80.5	98.6
Pa7	92	32701.0	72	20	4	4.8	78.3	99.9
Pa8	17	2998.8	7	10	1	2.0	41.2	99.9
Pa9	44	1555.3	30	14	2	2.3	68.2	99.9
Pa10	28	2700.0	21	7	0	0.0	75.0	100.0
Pa11	254	2136.4	228	26	26	36.6	89.8	98.3
Total	*924*	*30454.0*	*757*	*167*	*143*	*208.3*	*81.9*	*99.3*
Proposed method	Correct TP	Correct TN (times)	TP	FN	FP	FP (times)	Sens	Spec
Pa1	37	1457.9	36	1	12	19.5	97.3	98.7
Pa2	72	3286.6	69	3	1	1	95.8	100.0
Pa3	37	1089.0	34	3	4	5.6	91.9	99.5
Pa4	87	3646.9	74	13	8	9.5	85.1	99.7
Pa5	143	3335.9	127	16	26	29.6	88.8	99.1
Pa6	113	3686.3	101	12	7	6.4	89.4	99.8
Pa7	92	32701.0	76	16	0	0	82.6	100.0
Pa8	17	2998.8	9	8	0	0	52.9	100.0
Pa9	44	1555.3	37	7	0	0	84.1	100.0
Pa1	28	2700.0	21	7	1	1	75	100.0
Pa11	254	2136.4	233	21	17	17.6	91.7	99.2
Total	*924*	*30454.0*	*817*	*107*	*76*	*91.3*	*88.4*	*99.7*

TP: True positive; FN: False negative; FP: False positive; TN: True negative.
Sens: Sensitivity = TP/(TP + TN) × 100 (%).
Spec: Specificity = (1-FP/Correct TN) × 100 (%).

unlike what occurred with the previous method. It results from taking into account the wavelet coefficients. In Figure 4(*b*), the previous method did not detect apnea sufficiently because unstable respiratory waveforms contain intermittently high and low values. In contrast, our proposed method can detect the entire apnea

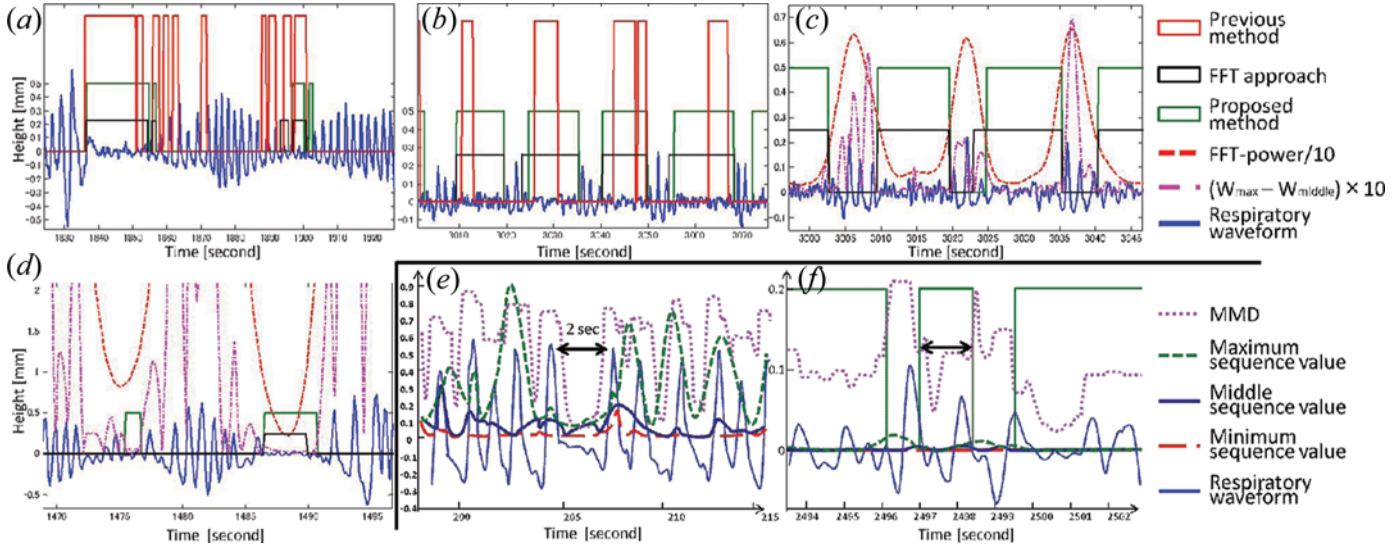

Figure 4. Results using our method, a previous method, the FFT approach, and the error sources. The period with a value of 0.5 shows the results of our method. That with a value of 0.25 also shows the results using FFT approach and the period with a value of 1.0 shows results using the previous method. (*a*) Results when the breathing cycle is long. (*b*) Results of unstable breathing. (*c, d*) FFT power–time series and the difference sequence value of wavelet coefficient of Equation (9) during a portion of CSR. Value of FFT power is divided by 10, and the value of $W_{max} - W_{middle}$ is multiplied by 10 for prominence in one figure. (*e*) False negative result due to a large gap in the wave height around the borders between the apnea and respiratory periods. (*f*) False-positive results due to low wave height. The period with a value of 0.2 shows the results of our method (color figure available online).

sequence with features of wavelet energy. It can diminish the number of false-positive and false-negative results. The results of the proposed method are superior to those of the previous method.

Although the FFT approach can detect apnea with few false- positive results, there are differences between tall and short waveforms (Figures 4(*a*) and 4(*b*)). FFT requires a certain length of time, or window, to extract energy from the respiratory frequency band. When the focal point is the period of apnea, this longer window causes extra frequency energy, which is extracted from the neighboring respiratory periods around the apnea. Therefore, the FFT has more influence on this phenomenon than the wavelet, and the proper threshold for FFT power is different depending on the wave height.

The advantage of the wavelet over FFT is not only detecting shorter apnea. It allows fewer false-positive results in case of a breath area around the apnea areas or a shorter respiratory period in CSR (Figure 4(*c*)). The value of the difference feature stably exceeds its threshold during respiratory period by extracting frequency energy from the local range of waveforms in the time axis. On the other hand, FFT power does not exceed its threshold during the respiratory period because of its fixed time window, which is comparatively long. Although the FFT approach does not have false-positive results with the MMD feature in this case, it seems that the wavelet is more stable than with FFT with regard to apnea detection. The influence of a fixed time window for FFT is shown in Figure 4(*d*). This approach cannot detect short apnea because of the extra frequency energy of the tall waveforms around the apnea. In Figures 4(*c*) and 4(*d*), the FFT power value is divided by 10, and the $W_{max} - W_{middle}$ value is multiplied by 10 because the FFT power value for prominence in one figure.

There were two factors mainly responsible for the false-negative results obtained using our proposed method. One is the 1–2 seconds of apnea (Figure 4(*e*)). The apnea duration is short, and the respiratory volume does not decrease near the apneic period. Therefore, the feature amount on the wavelet is higher than threshold. The other factor is a somewhat larger MMD value than at threshold. False-positive errors were mainly caused by the height (0.11–0.12 mm) of the respiratory waveform and the combination of low inspiration and low expiration periods (Figure 4(*f*)).

Our experiment proved that this method can reduce the influence of the trade-off regarding the threshold of the wavelet. Although errors have a common trade-off of the threshold on the difference feature of Equation (9), most errors take no more than 1–2 seconds. Hence, the proposed method reduces the influence of the trade-off on the threshold by combining the wavelet-based method and the MMD method. However, the proposed method is biased toward the wavelet-based method with respect to preventing detection errors. To reduce errors such as that in Figure 4(*c*), we should develop specialized features to obtain shape information for short apnea. Also, we should tighten the thresholds of our method for comparatively longer apnea.

5. CONCLUSIONS

We proposed a new method to detect apnea. The method can be applied to detecting CSR and estimating its severity. We believe that ultimately it can be used to develop a system whereby neonatal respiratory function can be evaluated.

The sensitivity of the proposed apnea detection method is 88.4%, and its specificity is 99.7%. We obtained these results by combining a wavelet-based method with an MMD method. The difference value of wavelet coefficients decreases during most apnea, and the MMD feature prevented the false-positive results of the difference feature. Although the MMD method could not detect apnea in the presence of unstable respiration, the method supports the wavelet-based method in cases in which the respiratory volume does not decrease near the period of apnea. The proposed method produces the combined results of the wavelet-based and MMD methods. These methods compensate for each other's weaknesses, and most errors take no more than 1–2 seconds. However, we need information about apnea whose duration is 1–2 seconds because some CSR includes apnea durations of 1–2 seconds. Apnea lasting >1.0 second is considered physiologically meaningful.

The technique for detecting apnea is biased toward the wavelet-based method using frequency information. Therefore, false-positive results are caused by the methods not containing accurate information on wave height. False-positive results are caused by trade-off of the thresholds for frequency energy. To solve this problem, we should consider waveform shape-based methods that include the correct wave height.

In the future, we plan to develop this apnea-based detection method so it can be used to extract features of CSR, such as apnea duration, durations of respiratory periods between apnea periods, and so on, using apnea information already obtained. We believe that the results of this study will contribute to our knowledge of respiratory physiology of the newborn.

REFERENCES

Chesson, A. L., R. A. Ferber, J. M. Fry, M. GriggDamber, K. M. Hartse, K. M. Hurwitz, S. Johnson, M. Littner, G. A. Kader, G. Rosen, R. B. Sangal, W. SchmidtNowara, and A. Sher. 1997. Practice parameters for the indications for polysomnography and related procedures. *Standards of Practice Committee of the American Sleep Disorders Association* 20: 406–422.

Finer, N. N., R. Higgines, J. Kattwinkel, and R. J. Martin. 2006. Summary proceedings from the apnea-of-prematurity group. *Official Journal of The Amerian Academy of Pediatrics* 117 (3): S47–S51.

Fontenla-Romero, O., B. Guijarro-Berdiñas, A. Alonso-Betanzos, and V. Moret-Bonillo. 2005. A new method for sleep apnea classification using wavelets and feedforward neural networks. *Artificial Intelligence in Medicine* 34 (1): 65–76.

Garde, A., B. F. Giraldo, R. Jane, I. Diaz, S. Herrer, S. Benito, M. Domingo, and A. Bayes-Genis. 2008. Characterization of periodic and non-periodic breathing pattern in chronic heart failure patients. *EMBS 2008 30th Annual International Conference of the IEEE* 30 (1): 3227–3230.

Garde, A., L. Sornmo, R. Jane, and B. F. Giraldo. 2011. Breathing pattern characterization in chronic heart failure patients using the respiratory flow signal. *Biomedical Engineering* 38 (12): 3572–3580.

Kelly, D. H. and D. C. Shannon. 1979. Periodic breathing in infants with near-miss sudden infant death syndrome. *Pediatrics* 63 (3): 355–360.

Kurami, Y., Y. Itoh, M. Natori, K. Ohzeki, and Y. Aoki. 2011. Development of non-contact respiratory monitoring system for newborn using a fg vision sensor. *IEEJ Trans* 130 (9): 1581–1587.

Lee, H., C. G. Rusin, D. E. Lake, M. T. Clark, L. Guin, T. J. Smoot, A. O. Paget-Brouwn, B. D. Vergales, J. Kattwinkel, J. R. Moorman, and J. B. Delos. 2012. A new algorithm for detecting central apnea in neonates. *Physiological Measurement* 33 (1): 1–17.

Nakano, H., T. Tanigawa, T. Furukawa, and S. Nishima. 2007. Automatic detection of sleep-disordered breathing from a single-channel airflow record. *European Respiratory Journal* 29 (4): 728–736.

Nakazawa, K., M. Nakajima, and H. Kobayashi. 1986. Development of 3-D shape measurement system using fiber grating. *IEICE Trans. Inf. & Syst* J-69-D (12): 1929–1935.

Oliveira, A. J., M. L. Nunes, A. Fojo-Olmos, F. M. Reisand, and J. C. da Costa. 2004. Clinical correlates of periodic breathing in neonatal polysomnography. *International Federation of Clinical Neurophysiology* 115 (10): 2247–2251.

Rigatto, H. and J. P. Brady. 1972. Periodic breathing and apnea in preterm infants. 2. Hypoxia as a primary event. *Pediatrics* 50 (2): 219–228.

Shannon, D. C., D. W. Carley, and D. H. Kelly. 1988. Periodic breathing: Quantitative analyses and clinical description. *Pediatr Pulmonology* 4 (2): 98–102.

Tian, J. and J. Liu. 2005. Apnea detection based on time delay neural network. *Engineering in Medicine and Biology 27th Annual Conference* 27 (3): 2571–2574.

van Houdt, P. J., P. P. W. Ossenblock, M. G. van Erp, K. E. Schreuder, R. J. J. Krijn, P. A. J. M. Boon, and P. J. M. Cluitmans. 2011. Automatic breath-to-breath analysis of nocturnal polysomnographic recordings. *International Federation for Medical and Biolgical Engineering* 49 (7): 819–830.

Varady, P., T. Micsik, S. Benedek, and Z. Benyo. 2002. A novel method for the detection of apnea and hypopnea events in respiration signals. *IEEE Transactions on Biomedical Engineering* 49 (9): 936–942.